Theoretical Modeling of Putative Ni(III)−F_{430} Intermediates of Methylcoenzyme M Reductase

Tebikie Wondimagegn[†] and Abhik Ghosh*[,†,‡]

Institute of Chemistry, University of Tromsø
N-9037 Tromsø, Norway

Received May 30, 2000
Revised Manuscript Received December 19, 2000

Methycoenzyme M reductase (MCR)[1,2] catalyzes the last chemical step of methane formation by methanogenic organisms (methanoarchaea), the reaction involving a two-electron reduction of a methylthioether, coenzyme M ($CH_3-S-CoM$), by *N*-7-mercaptoheptanoyl-threonine phosphate (CoB−SH). A key component of the active site of MCR is F_{430} (Scheme 1) a nickel tetrapyrrole cofactor, whose Ni(I) form is present in the active form of the enzyme, MCR_{red1}.[1,2] On the basis of high-resolution X-ray crystallographic structures of two EPR-silent high-spin Ni(II) forms of the inactive enzyme, Ermler and co-workers[3] proposed the mechanism shown in Scheme 1. The mechanism provokes the question whether the tetrapyrrole ligand of F_{430}, which is unusual in its ability to stabilize low-valent Ni(I) in a nitrogen-only ligand environment, can also give rise to high-valent Ni(III) intermediates. We present here density functional theory (DFT) calculations[4,5] that suggest that the answer is "yes". In addition, other inactive EPR-visible $S = {}^1/_2$ states of MCR are known, known as ox1 and ox2, for which either Ni(I) (d^9) or Ni(III) (d^7) formulations are conceivable.[1,6,7] A limited attempt is also reported here on the theoretical modeling of these states.

Scheme 1

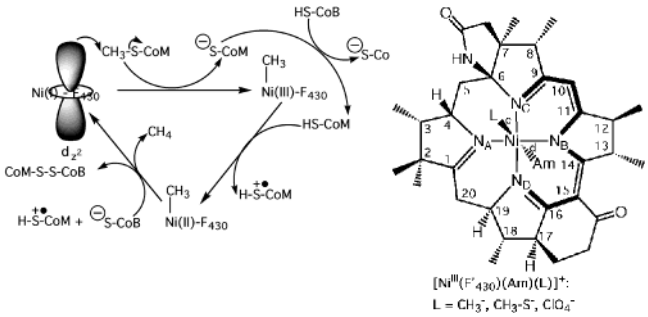

Table 1. Selected Optimized Distances (Å), Atomic Charges, and Spin Populations of Ni(III)−F'_{430} Complexes[a]

Distances

cmpd	Ni−N_A	Ni−N_B	Ni−N_C	Ni−N_D	c	d
$[Ni^{III}(F'_{430})(ClO_4)(Am)]^+$	2.08	2.01	2.01	1.96	2.12 (O)	*c*
$[Ni^{III}(F'_{430})(CH_3)(Am)]^+$	2.21	2.13	2.01	2.00	1.96 (C)	2.20
$[Ni^{III}(F'_{430})(SCH_3)(Am)]^+$	2.20	2.10	1.97	1.96	2.34 (S)	2.42

Charge

cmpd	N_A	N_B	N_C	N_D	Ni	L[b]
$[Ni^{III}(F'_{430})(ClO_4)(Am)]^+$	−0.3433	−0.4326	−0.3763	−0.4052	0.5630	−0.5765
$[Ni^{III}(F'_{430})(CH_3)(Am)]^+$	−0.3396	0.4112	−0.3921	−0.4047	0.6275	0.4108
$[Ni^{III}(F'_{430})(SCH_3)(Am)]^+$	-0.3415	-0.4238	-0.3762	-0.3902	0.5107	0.0222

Spin Populations

cmpd	N_A	N_B	N_C	N_D	Ni	L[b]
$[Ni^{III}(F'_{430})(ClO_4)(Am)]^+$	0.0052	0.0309	0.0353	0.0167	0.5707	0.1880
$[Ni^{III}(F'_{430})(CH_3)(Am)]^+$	0.0795	0.0933	0.0486	0.0578	0.7685	−0.0814
$[Ni^{III}(F'_{430})(SCH_3)(Am)]^+$	0.0885	0.0842	−0.0032	0.0081	0.6546	0.1353

[a] Some relevant symbols are explained in Scheme 1. [b] The charge or spin population refers to the atom in the axial ligand (other than Am) that is directly bonded to the nickel atom. [c] In these compounds, the Am ligand fell off the nickel atom in the course of geometry optimization.

In this work, we simulate various putative Ni(III) derivatives of the natural F_{430} cofactor by a relatively "high-fidelity" model complex designated F'_{430} (Scheme 1). The F'_{430} complexes are "derived" from natural F_{430} by replacement of all peripheral alkyl substituents by methyl groups. Here we report calculated DFT results on three Ni(III)-F'_{430} complexes with ClO_4^-, CH_3, and CH_3-S^- axial ligands, the sixth ligand in each case being *O*-bound acetamide (Am). The CH_3-S^- and Am ligands are intended to model the coenzyme M thiolate (CoM-S^-) and Gln147 axial ligands, respectively, found in the crystal structure of $MCR_{ox1-silent}$.[3] In a recent paper, we have presented analogous DFT calculations on four-coordinate Ni(I) and low-spin Ni(II) F'_{430} and 12,13-diepi-F'_{430} complexes.[8]

A key result of this study is that the singly occupied MOs of the model complexes $[Ni^{III}(F'_{430})(ClO_4)(Am)]^+$ and $[Ni^{III}(F'_{430})(CH_3)(Am)]^+$ are very different in terms of their spatial distribution and essentially correspond to Ni d_{z^2} and $d_{x^2-y^2}$ orbitals, respectively. As shown in Table 1, the Ni unpaired electron spin population in $[Ni^{III}(F'_{430})(ClO_4)(Am)]^+$ is approximately 0.57, with the remainder of the electronic spin distributed over the axial ligands. In contrast, the Ni unpaired electron spin population in $[Ni^{III}(F'_{430})(CH_3)(Am)]^+$ is approximately 0.77, and the remainder of the unpaired spin is distributed roughly equally on the four nitrogens of the F'_{430} ligand. The Ni spin population in the Ni(III)−CH_3 case is surprisingly similar to a value of 0.83 found earlier for Ni(I)−F'_{430},[8] a result that may be relevant to areas of nickel chemistry, not specifically connected to MCR and cofactor F_{430}. Thus, Ni(III) complexes with the unusual "t_{2g}"$^6(x^2 - y^2)^1$ electronic configuration may simulate Ni(I) in terms of their electronic spin density profiles and EPR parameters. The different electronic configurations of $[Ni^{III}(F'_{430})(ClO_4)(Am)]^+$ and $[Ni^{III}(F'_{430})(CH_3)(Am)]^+$ are reflected in significant differences in coordination geometry of the nickel center. In the Ni(III)−ClO_4 case, the Ni−N distances are 1.96−2.08 Å. In the Ni(III)−CH_3 case, the Ni−N distances are significantly longer, 2.00−2.21 Å, as expected on the basis of occupancy of the Ni $d_{x^2-y^2}$ orbital.

These results are in generally good agreement with relevant experimental results. For example, Jaun generated Ni(III)−$F_{430}Me_5$ electrochemically in acetonitrile and observed an EPR spectrum characteristic for a tetragonally distorted $S = {}^1/_2$ system

† University of Tromsø. Address correspondence to A.G. at the University of Tromsø. Email: abhik@chem.uit.no.
‡ Additional affiliation: San Diego Supercomputer Center, LaJolla, CA 92093.

(1) Thauer, R. K. *Microbiology* **1998**, *144*, 2377.
(2) Telser, J. *Struct. Bonding* **1998**, *91*, 31.
(3) Ermler, U.; Grabarse, W.; Shima, S.; Goubeaud, M.; Thauer, R. K. *Science* **1997**, *278*, 1457.
(4) The calculations were carried out with the ADF program system, the PW91 functional, Slater-type triple-ζ plus polarization basis sets, a fine mesh for numerical evaluation of electron repulsion integrals, and tight convergence criteria for atomic forces and displacements in the geometry optimizations, and a Cray Origin 2000 computer. The ADF program is obtainable from: Scientific Computing and Modelling, Department of Theoretical Chemistry, Vrije Universiteit, 1081 HV Amsterdam, The Netherlands.
(5) For recent reviews of DFT studies of the molecular structures of porphyrins and metalloporphyrins, see: (a) Ghosh, A. In *The Porphyrin Handbook*; Kadish, K. M., Smith, K. M., Guilard, R., Eds.; Academic: New York, 2000; Vol. 7, Chapter 47, pp 1−38. (b) Ghosh, A. *Acc. Chem. Res.* **1998**, *31*, 189.
(6) Goubeaud, M.; Schreiner, G.; Thauer, R. *Eur. J. Biochem.* **1997**, *23*, 110.
(7) Albracht, S. P. J.; Ankel-Fuchs, D.; Böcher, R.; Ellermann, J.; Moll, J.; van der Zwaan, J. W.; Thauer, R. K. *Biochim. Biophys. Acta* **1986**, *955*, 86.
(8) Wondimagegn, T.; Ghosh, A. *J. Am. Chem. Soc.* **2000**, *122*, 6375.

10.1021/ja001870j CCC: $20.00
Published on Web 01/24/2001

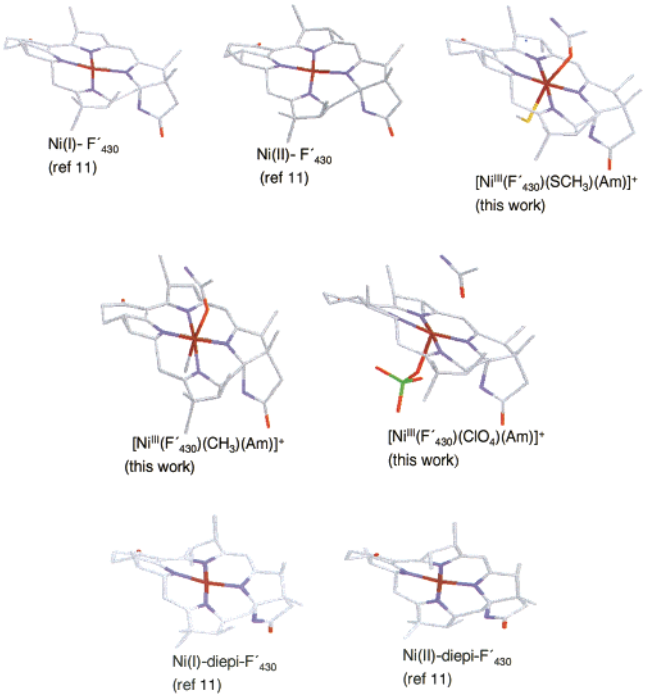

Figure 1. Stick representation of the optimized geometries of various F'_{430} complexes. Hydrogen atoms are omitted for clarity.

with a $(z^2)^1$ ground state ($g = 2.020$, $g = 2.211$),[9] consistent with our finding of a $(z^2)^1$ ground state for $[Ni^{III}(F'_{430})(ClO_4)(Am)]^+$. Similarly, Bocian and co-workers have reported EPR evidence[10] for the existence of Ni(III) tetrapyrrole complexes with unusual "t_{2g}"$^6(x^2 - y^2)^1$ electronic configurations. Thus, these researchers found a typical $(z^2)^1$-type Ni(III) EPR spectrum for $[Ni(TPP)(Py)_2]^+$ but a very different spectrum for $[Ni(TPP)(CN)_2]^-$ (TPP = tetraphenylporphyrin), which they assigned to an $(x^2 - y^2)^1$ d-occupancy. DFT calculations from our laboratory supported the conclusions reached by Bocian and co-workers. Using the unsubstituted porphyrin ligand (P) in our DFT calculations, we found that the $(z^2)^1$ configuration of $[Ni(P)(Py)_2]^+$ was favored over the $(x^2 - y^2)^1$ configuration by 0.43 eV, but for $[Ni(TPP)(CN)_2]^-$, the energy ordering was reversed with the $(x^2 - y^2)^1$ configuration favored by 0.96 eV.[11] Thus, the very strongly σ-donating methyl ligand in $[Ni^{III}(F'_{430})(CH_3)(Am)]^+$ and the cyanide ligands in $[Ni(TPP)(CN)_2]^-$ discourage occupancy of the d_{z^2} orbital and favor occupancy of the $d_{x^2-y^2}$ orbital instead. The optimized nickel−ligand bond distances in $[Ni(P)(Py)_2]^+$ versus $[Ni(TPP)(CN)_2]^-$ exhibited the same qualitative differences as those found here for $[Ni^{III}(F'_{430})(ClO_4)(Am)]^+$ and $[Ni^{III}(F'_{430})(CH_3)(Am)]^+$ (Table 1).

In a recent DFT study of the Ni(I) and low-spin Ni(II) states of F'_{430} and 12,13-diepi-F'_{430}, we have shown that the F_{430} ligand exhibits unique conformational characteristics, very different from its thermodynamically more stable 12,13-diepimer and from other hydroporphyrins. Figure 1, which presents stick diagrams of all the F'_{430} and 12,13-diepimeric structures optimized in our laboratory until now, clearly shows that the F'_{430} complexes are significantly less ruffled than the diepimeric structures. Steric interactions involving the 12- and 13-substituents and the methine hydrogen at the 10-position exercise a significant planarizing force on the F_{430} macrocycle and discourage it from strong ruffling. This may be a factor that stabilizes the Ni(I) oxidation state. We wrote[11] that Nature appears to have "specifically tailored the molecular architecture of F_{430} for occupancy of the nickel $d_{x^2-y^2}$ orbital and for relatively long Ni−N bonds". In light of the above results, it is tempting to propose that this may indeed be an important principle of F_{430} chemistry: the viability of the putative Ni(II)−CH_3 and Ni(III)−CH_3 intermediates of F_{430} should also depend critically on occupancy of the nickel $d_{x^2-y^2}$ orbital.

We also attempt here to briefly address the controversial assignment of the nickel oxidation states of the EPR-visible inactive ox1 and ox2 states of MCR. The less reducing conditions necessary for generating the ox states, relative to red1, and the fact that the reductant Ti(III) citrate converts ox1 to red1 suggest that ox1 is Ni(III).[1,6,7] However, the ox1 and ox2 states[12] exhibit the same EPR *g*-value pattern and ^{14}N ENDOR hyperfine coupling as red1 and Ni(I)−F_{430},[13] indicating a metal $(x^2 - y^2)^1$ electronic configuration. On the basis of this finding and a variety of other considerations, the authors of the magnetic resonance study concluded that ox1 and ox2 are Ni(I), not Ni(III). To us, this conclusion did not seem to be entirely convincing: what if a CoM−S−Ni(III)−F_{430} species also has an $(x^2 - y^2)^1$ configuration and simulates the EPR behavior of Ni(I)? Our calculated results on the model complex $[Ni(F'_{430})(SMe)(Am)]^+$ permit a partial evaluation of these different electronic-structural scenarios.

Our calculated results on $[Ni(F'_{430})(SMe)(Am)]^+$ support the suggestion, on the basis of considerations of EPR *g*-values and hyperfine couplings,[12] that a description of ox1 in terms of a high-spin Ni(II) center spin-coupled to a sulfur radical is not reasonable. The optimized geometry of $[Ni(F'_{430})(SMe)(Am)]^+$ reveals long Ni−N distances, consistent with occupancy of the Ni $d_{x^2-y^2}$ orbital. However, the unpaired spin profile is qualitatively unlike that in Ni(I)−F'_{430}, $[Ni^{III}(F'_{430})(ClO_4)(Am)]^+$ or $[Ni^{III}(F'_{430})(CH_3)(Am)]^+$, with the main contributions as follows: Ni (65%), S (14%), and two opposite nitrogen atoms, N_A and N_B (8−9%, each). The open-shell orbital resulting in this spin-density distribution involves metal−ligand π-bonding and may be schematically represented as follows:[14]

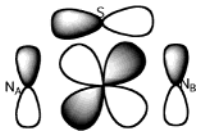

In conclusion, DFT calculations provide a simple explanation of how MCR might achieve the somewhat paradoxical stabilization of both low-valent Ni(I) and high-valent, formally Ni(III)−methyl intermediates, the key factor in each case being the facile occupancy of the Ni $d_{x^2-y^2}$ orbital. Second, the calculations show that the electronic spin density profiles of $(x^2 - y^2)^1$-type Ni(III) species can be deceptive and closely mimic those of Ni(I) species, a result that may be of relevance to other areas of nickel chemistry such as the chemistry [NiFe] hydrogenases.[15] Third, the $(x^2 - y^2)^1$-type EPR and ^{14}N ENDOR spectra of MCR ox1 and ox2 appear not to be compatible with the spin density profile of an F_{430}−Ni(III)−thiolate model complex, in agreement with conclusions reached by Hoffman, Ragsdale, and co-workers.[12]

Acknowledgment. We acknowledge support from the Norwegian Research Council and the VISTA Grant of Statoil (Norway) and discussions with Profs. Brian Hoffman and David Bocian.

Supporting Information Available: Table S1 gives ruffling dihedral angles for the different molecules studied. Atomic Cartesian coordinates in Å are given for each optimized geometry (PDF). This material is available free of charge via the Internet at http://pubs.acs.org.

JA001870J

(9) Jaun, B. *Helv. Chim. Acta* **1990**, *73*, 2209.
(10) Seth, J.; Palaniappan, V.; Bocian, D. F. *Inorg. Chem.* **1995**, *34*, 2201.
(11) Ghosh, A.; Wondimagegn, T.; Gonzalez, E.; Halvorsen, I. *J. Inorg. Biochem.* **2000**, *78*, 79.
(12) Telser, J.; Horng, Y.-C.; Becker, D. F.; Hoffman, B. M.; Ragsdale, S. W. *J. Am. Chem. Soc.* **2000**, *122*, 182.
(13) Telser, J.; Fann, Y.-C.; Renner, M. W.; Fajer, J.; Wang, S.; Zhang, H.; Scott, R. A.; Hoffman, B. M. *J. Am. Chem. Soc.* **1997**, *119*, 733.
(14) The metal electronic configuration may be approximately described as $(xy)^2(yz)^2(x^2 - y^2)^2(xz)^1$, where the *xy* plane may be identified with the mean N_4 plane and the *xz* plane with the plane containing the Ni, S, N_A, and N_B atoms.
(15) (a) Maroney, M. J. *Curr. Opin. Chem. Biol.* **1999**, *3*, 188. (b) Ragsdale, S. W. *Curr. Opin. Chem. Biol.* **1998**, *2*, 208.